

figuration selection is less severe than that of basis set truncation, it is clear that only the smaller truncation thresholds provide acceptable agreement with the SOCI results.

Based on these findings it seems that rather accurate results for  $N_2^{2+}$  can be obtained by using a [4s 3p 2d 1f] basis set and MRCI with a selection threshold of 0.025 or less. The very large near-degeneracy observed for many states argues strongly for a multiconfigurational treatment from the outset: when CASSCF calculations are used to define the MO space for the CI calculation the ordering of states is generally close to the SOCI or MRCI ordering, which is not the case for SCF wave functions.<sup>8</sup> It should be possible to obtain high accuracy by performing a single CASSCF calculation on an average of states of the same spin and symmetry type, followed by a single MRCI calculation for all desired states of this type. Such an approach has been shown to agree very well with full CI results for excitation and ionization energies.<sup>19</sup>

## Conclusions

The spectroscopic constants of low-lying states of  $N_2^{2+}$  have been computed by using extended basis sets and SOCI wave functions. The ground state is definitively shown to be  $^1\Sigma_g^+$ , while the computed  $T_e$  for the  $^1\Sigma_u^+ - ^1\Sigma_g^+$  transition, which should be labeled D  $\leftrightarrow$  X, agrees with high-resolution optical measurements to within about 0.1 eV. Selection of reference CSFs is shown to give agreement with the SOCI results only when small selection thresholds are used.

*Acknowledgment.* We acknowledge the support provided by the NAS Facility. Helpful discussions with C. W. Bauschlicher and S. R. Langhoff are gratefully acknowledged.

Registry No.  $N_2^{2+}$ , 12192-19-7.

(19) Bauschlicher, C. W.; Taylor, P. R. *J. Chem. Phys.* 1987, 86, 2844.

## Ab Initio Studies of the Structure and Energetics of the $H^-(H_2)$ Complex

Grzegorz Chalasiński,

Department of Chemistry, University of Utah, Salt Lake City, Utah 84112, and Department of Chemistry, University of Warsaw, 02-093 Warsaw, Poland<sup>†</sup>

Rick A. Kendall, and Jack Simons\*

Department of Chemistry, University of Utah, Salt Lake City, Utah 84112 (Received: April 21, 1987)

The  $H^-(H_2)$  complex is examined by using various levels of Møller-Plesset perturbation theory (MPPT). Ab initio interaction energies are calculated through fourth-order MPPT (MP4) by using large and flexible basis sets. Our best atomic orbital basis yields an attractive interaction energy, relative to  $H_2$  and  $H^-$ , of  $\sim 1.2$  kcal/mol at the MP4 level, but proper accounting of zero-point vibrational energies shows that  $H^-(H_2)$  is thermodynamically unstable. The importance of correcting for basis set superposition error is demonstrated. Analytically optimized geometries at the SCF and MP2 levels and pointwise geometry optimizations with basis set superposition corrections are reported. The weak vibrational stretching mode of the  $H^-$  in the complex is also investigated. The potential energy surface along this mode supports six vibrational levels. SCF harmonic frequencies are reported for all vibrational modes. The corresponding stretching modes of the isotopically substituted complexes  $H^-(HD)$  and  $D^-(H_2)$  are also analyzed. The potential energy surface crossings between  $H^-(H_2)$  and the neutral  $H_3$  at pertinent geometries are shown, and their relevance to electron detachment in  $H_2 + H^-$  collisions is discussed.

### I. Introduction

There has been an interest in the study of hydrogen ion clusters. However, only positive clusters,  $H_n^+$ , where  $n = 3, 5, 7, \dots$ , have been discovered<sup>1</sup> and successfully analyzed by means of both experimental<sup>2</sup> and ab initio theoretical methods (cf. Hirao and Yamabe<sup>3</sup> and references cited therein). Substantially weaker  $H_n^-$  complexes, where  $n = 3, 5, 7, \dots$ , have so far eluded experimental determination. Yet, it has been argued that the extreme conditions in gaseous nebulae may be suitable for weakly bound negative ion clusters to exist.<sup>4,5</sup> It is, in fact, possible that some diffuse interstellar absorption lines are due to vibrational structure in the electronic transitions of  $H_n^-$ .

So far, theoretical calculations have predicted the stabilization of  $H_n^-$ , in particular of  $H^-(H_2)$ , to be less than 1 kcal/mol,<sup>3,5</sup> which may not be strong enough to support a vibrational level.<sup>3</sup> In addition, as a very weak van der Waals complex,  $H^-(H_2)$  proves to be quite challenging to ab initio calculations. In earlier theoretical studies, the problem of dealing with a large basis set superposition error (BSSE) turned out to be serious even at the SCF level due to the diffuse character of the  $H^-$  electron charge cloud.<sup>5</sup> To make matters worse, BSSE is usually much worse at the correlated level.<sup>6,7</sup> Finally, the CI-SD method used in the previous calculations is size-inconsistent, and the size-consistency

Davidson correction<sup>8</sup> turned out to be very significant.<sup>3</sup>

The aim of this paper is to provide advanced calculations on the ground electronic state of the  $H^-(H_2)$  complex, the simplest of the  $H_n^-$ ,  $n = 3, 5, \dots$  sequence. An inherently size-consistent method, Møller-Plesset perturbation theory (MPPT)<sup>9</sup> through the fourth order (MP4), was used to allow for electron correlation effects. Optimization of geometry at the SCF and MP2 levels was carried out with and without BSSE corrections. Several fairly large basis sets were used, and our best results are only slightly affected by BSSE. The results with smaller basis sets are also shown to be reliable but only when the CP method<sup>10</sup> is used to

- (1) Clappitt, R.; Gowland, L. *Nature (London)* 1969, 223, 815.
- (2) Hiraoka, K.; Kebarle, P. *J. Chem. Phys.* 1975, 62, 2267.
- (3) Hirao, K.; Yamabe, S. *Chem. Phys.* 1983, 80, 237.
- (4) Sapse, A. M.; Rayez-Meaume, M. T.; Rayez, J. C.; Massa, L. J. *Nature (London)* 1979, 278, 332.
- (5) Rayez, J. C.; Rayez-Meaume, M. T.; Massa, L. J. *J. Chem. Phys.* 1981, 75, 5393.
- (6) Van Lenthe, J. H.; van Dam, T.; van Duijneveldt, F. B.; Kroon-Batenburg, L. M. *J. Faraday Symp. Chem. Soc.* 1984, 19, 125.
- (7) Gutowski, M.; van Lenthe, J. H.; Verbeek, J.; van Duijneveldt, F. B.; Chalasiński, G. *Chem. Phys. Lett.* 1986, 124, 370.
- (8) Davidson, E. R. In *The World of Quantum Chemistry*; Daudel, R.; Pullman, B., Eds.; Reidel: Dordrecht, 1974; p 17.
- (9) Binkley, J. S.; Pople, J. A. *Int. J. Quantum Chem.* 1975, 9, 229.
- (10) Krishnan, R.; Frisch, M. J.; Pople, J. A. *J. Chem. Phys.* 1980, 72, 4244.

<sup>†</sup> Permanent address.

TABLE I: Basis Sets Used for the H<sup>-</sup>(H<sub>2</sub>) System<sup>a</sup>

label	basis	exponents		H <sub>2</sub>	H <sup>-</sup>
M	6s[4s] 2p 1d	van Duijneveldt; <sup>21</sup> 5s [311] + diffuse 1s(0.03) 0.75, 0.25 0.075; Diercksen & Sadlej <sup>23</sup>	HF	-1.132 567	-0.487 480
			MP2	-1.161 520	-0.512 334
			MP4	-1.169 240	-0.521 828
L	7s[4s] 2p 1d 1f	Diercksen & Sadlej <sup>23</sup> 0.07; Meyer <sup>24</sup>	HF	-1.131 893	-0.487 517
			MP2	-1.160 015	-0.512 802
			MP4	-1.167 571	-0.522 675
N	9s[5s] 4p	Lie & Clementi; <sup>25</sup> 8s [5111] + diffuse 1s(0.017 247 8) <sup>b</sup> 2.273 471, 0.841 306, 0.293 257, 0.085 31 <sup>b</sup>	HF	-1.133 545	-0.487 787
			MP2	-1.163 907	-0.514 361
			MP4	-1.171 318	-0.524 655
N(d)	as N basis + 1d(0.075)		HF	-1.133 545	-0.487 787
			MP2	-1.163 931	-0.514 869
			MP4	-1.171 338	-0.524 728
N(3d)	as N(d) basis + 2d(0.2, 0.7) d exponents of Meyer <sup>24</sup>		HF	-1.133 555	-0.487 787
			MP2	-1.165 568	-0.516 555
			MP4	-1.172 559	-0.525 503
N(3df)	as N(3d) basis + 1f(0.07) f exponent of Meyer <sup>24</sup>		HF	-1.133 555	-0.487 787
			MP2	-1.165 575	-0.516 633
			MP4	-1.172 563	-0.525 496
accurate results			HF	-1.133 63 <sup>c</sup>	-0.487 927 <sup>d</sup>
			CI	-1.174 47 <sup>e</sup>	-0.527 751 <sup>f</sup>

<sup>a</sup>  $r_{\text{HH}} = 0.739 \text{ \AA}$ . For the sake of convenience all bases are given explicitly in Table VI. Energies in hartrees, exponents in  $a_0^{-2}$ . <sup>b</sup> Optimized by Adams<sup>26</sup> for the correlation energy of H<sub>2</sub> and H<sup>-</sup> simultaneously. <sup>c</sup> Davidson and Jones.<sup>35</sup> <sup>d</sup> Froese Fischer, p 165.<sup>37</sup> <sup>e</sup> Kolos and Wolniewicz.<sup>36</sup> <sup>f</sup> Pekeris.<sup>38</sup>

correct for BSSE. The stabilization of H<sup>-</sup>(H<sub>2</sub>) with respect to H<sup>-</sup> + H<sub>2</sub> was found to be ca. 1.2 kcal/mol, and the potential surface supports six "stretching" vibrational levels. The H<sup>-</sup>(H<sub>2</sub>) minimum on the potential hypersurface, as is typical for anion-molecule complexes, is quite broad (i.e., has small local force constants). The equilibrium H<sup>-</sup>-H<sub>2</sub> distance  $R_e$  optimized at the SCF level differs by ca. -0.4 Å from  $R_e$  optimized at the correlated level, but the difference in BSSE-corrected binding energy at these two points does not exceed 0.1 kcal/mol. The addition of zero-point vibrational energies shows that H<sup>-</sup>(H<sub>2</sub>) is thermodynamically unstable. The complex will break apart into the H<sub>2</sub> and H<sup>-</sup> moieties.

## II. Method

Calculations of intermolecular interactions by means of MPPT offers several advantages in comparison with other methods. As shown by Diercksen et al. on the demanding Be<sub>2</sub> system,<sup>11</sup> a complete fourth-order MPPT calculation may recover a sufficient portion of the pertinent correlation effects, leading, at the same time, to size-consistent results. Very high order and highly accurate calculations of Handy et al.<sup>12</sup> confirmed that, unless multiconfigurational bond breaking or curve crossings occur, the MPPT series is well convergent and thus quite reliable. Furthermore, many valuable qualitative and even quantitative results may be already obtained at lower than the fourth-order level by using standard basis sets. As shown by Kestner et al.<sup>13</sup> and by Szczesniak and Scheiner,<sup>14</sup> if BSSE is corrected for, the MP2 and MP3 levels can successfully be applied to study hydrogen-bonded systems. It should be emphasized here that because of relatively simple expressions for  $E_{\text{MP}}^{(2)}$  and  $E_{\text{MP}}^{(3)}$ , the pertinent computer codes can be easily vectorized to yield a high performance on supercomputers and applied even for such large systems as the nitromethane dimer.<sup>15</sup> It is also important to note that the second-

and third-order corrections to the interaction energy may asymptotically be related to the physically meaningful contributions to the interaction energy derived from the classic Rayleigh-Schrödinger (RS) perturbation theory of intermolecular forces.<sup>16</sup>

The method used in the calculations presented in this paper is the complete fourth-order MPPT, implemented in the Gaussian 82 computer codes.<sup>17,18</sup> All contributions to the total energy through fourth order in the electron correlation perturbation series (i.e., those due to single (S), double (D), triple (T), and quadruple (Q) substitutions relative to the reference Hartree-Fock determinant) are included. The interaction energy at the  $i$ th order is defined as

$$\Delta E^{(i)} = E_{\text{AB}}^{(i)} - E_{\text{A}}^{(i)} - E_{\text{B}}^{(i)} \quad (1)$$

where  $E_{\text{AB}}^{(i)}$ ,  $E_{\text{A}}^{(i)}$ , and  $E_{\text{B}}^{(i)}$  are the  $i$ th-order MPPT energies of AB, A, and B, respectively. The interaction energy through the  $i$ th order may be defined in like fashion:

$$\Delta E(i) = E_{\text{AB}}(i) - E_{\text{A}}(i) - E_{\text{B}}(i) \quad (2)$$

where  $E_{\text{AB}}(i)$ ,  $E_{\text{A}}(i)$ , and  $E_{\text{B}}(i)$  are the MPPT energies through the  $i$ th order of AB, A, and B, respectively (e.g.,  $\Delta E_x(i) = \sum_{j=1}^i \Delta E_x^{(j)}$ ). Note that the Hartree-Fock (HF) interaction energy is given in terms of the zero- and first-order energies as

$$\Delta E^{\text{SCF}} = \Delta E(0) + \Delta E(1) \quad (3)$$

When the energies of A, B, and AB are calculated with finite basis sets ( $\chi_{\text{A}}$ ,  $\chi_{\text{B}}$ , and  $\chi_{\text{A}} \cup \chi_{\text{B}}$ , respectively) the use of eq 1 and 2 involves BSSE problems. To circumvent this apparent basis set inconsistency, the "counterpoise" (CP) method was set forth by Boys and Bernardi.<sup>10</sup> The CP method consists in the calculation of the energies of AB, A, and B in the same  $\chi_{\text{A}} \cup \chi_{\text{B}}$  basis. The BSSE in the  $i$ th order of MPPT is then defined as

$$\delta_{\text{A}}^{(i)} = E_{\text{A}}^{(i)}(\chi_{\text{A}} \cup \chi_{\text{B}}) - E_{\text{A}}^{(i)}(\chi_{\text{A}}) \quad (4)$$

and similarly for B. Since the pioneering work of Boys and Bernardi, a large body of evidence has been collected to support the usefulness of the CP method (cf. the recent review by van

(10) Boys, S. F.; Bernardi, F. *Mol. Phys.* **1970**, *19*, 553.

(11) Diercksen, G. H. F.; Kello, V.; Sadlej, A. J. *Chem. Phys.* **1985**, *96*, 59.

(12) Handy, N. C.; Knowles, P. J.; Somasundram, K. *Theor. Chim. Acta* **1985**, *68*, 87. Knowles, P. J.; Somasundram, K.; Handy, N. C. *Chem. Phys. Lett.* **1986**, *113*, 8.

(13) Newton, M. D.; Kestner, N. R. *Chem. Phys. Lett.* **1983**, *94*, 198. Kestner, N. R.; Newton, M. D.; Mathers, T. L. *Int. J. Quantum Chem.* **1983**, *S17*, 431.

(14) Szczesniak, M.; Scheiner, S. *J. Chem. Phys.* **1986**, *84*, 6328.

(15) Cole, S. J.; Szalewicz, K.; Purvis, G. D., III; Bartlett, R. J. *J. Chem. Phys.* **1986**, *84*, 6833. Cole, S. J.; Szalewicz, K.; Bartlett, R. J. *Int. J. Quantum Chem.* **1986**, *30*, 695.

(16) Chalański, G.; Szczesniak, M., to be published.

(17) Binkley, J. S.; Whiteside, R. A.; Krishnan, R.; Seeger, R.; DeFrees, D. J.; Schlegel, H. B.; Topiol, S.; Kahn, L. R.; Pople, J. A. *QCPE* **1983**, *13*, program 406.

(18) Binkley, J. S.; Frisch, M. J.; DeFrees, D. J.; Raghavachari, K.; Whiteside, R. A.; Schlegel, H. B.; Fluder, E. M.; Pople, J. A. *Gaussian 82*; Carnegie-Mellon University; Pittsburgh, PA, 1986.

**TABLE II: Interaction Energy between  $\text{H}^-$  and  $\text{H}_2$ , Linear Configuration (cf. Figure 1), at SCF, MP2, and MP4 Levels, Calculated with M Basis (Three Points Also with N(3d) Basis)<sup>a</sup>**

basis	method	R									
		2.731	3.031	3.148	3.181	3.231	3.281	3.331	3.551	3.931	4.231
M	SCF	+0.0017 (-0.0607)	-1.0112 (-1.070)	-1.209 (-1.266)	-1.249 (-1.306)	-1.302 (-1.359)	-1.345 (-1.400)	-1.378 (-1.433)	-1.436 (-1.489)	-1.346 (-1.393)	-1.207 (-1.250)
M	MP2	-1.311 (-2.380)	-1.798 (-2.785)	-1.852 (-2.811)	-1.857 (-2.809)	-1.860 (-2.800)	-1.857 (-2.785)	-1.848 (-2.763)	-1.759 (-2.617)	-1.516 (-2.262)	-1.310 (-1.959)
N(3d)				-1.977 (-2.105)	-1.979 (-2.105)	-1.974 (-2.096)					
M	MP4	-1.180 (-2.399)	-1.677 (-2.831)	-1.737 (-2.865)	-1.744 (-2.865)	-1.751 (-2.859)	-1.751 (-2.846)	-1.745 (-2.827)	-1.673 (-2.689)	-1.456 (-2.336)	-1.266 (-2.028)
N(3d)				-1.838 (-1.865)	-1.843 (-1.869)	-1.844 (-1.869)					

<sup>a</sup>The CP-uncorrected values are given in parentheses. All energies in mhartrees; distances in angstroms.

Lenthe et al.<sup>19</sup>). As to whether the CP method overcorrects the actual BSSE, a number of both theoretical and numerical arguments have been recently presented by Gutowski et al.<sup>7,20</sup> and tend to support the original CP approach of Boys and Bernardi over any alternatives yet put forth. In the present work, this version of the CP method was used to handle BSSE difficulties.

### III. Results and Discussion

**A. Basis Sets.** The contracted Gaussian type orbital (GTO) basis sets used in this work are described in Table I, and for the sake of convenience we also tabulated them explicitly in Table VI. The related energies of  $\text{H}_2$  and  $\text{H}^-$  at the SCF, MP2, and MP4 levels are provided in Table I also. The three different bases correspond to three different "philosophies" of design. Basis M is an energetically optimized basis of the "TZ + diffuse + polarization" type. Basis L was optimized with the  $\text{H}_2$  electric properties in mind. Finally, bases N were energetically optimized with the p-symmetry subset optimized for the electron correlation of  $\text{H}_2$  and  $\text{H}^-$ .

**Basis M.** The core of the M basis is the variationally optimized 5s CGTO set from van Duijneveldt's tables.<sup>21</sup> To this set the following has been added: (a) an additional diffuse 1s orbital, with an exponent of 0.03 suggested by Clark et al.<sup>22</sup> to improve the description of  $\text{H}^-$ ; and (b) polarization functions, two p type and one d-type function.

**Basis L.** The "spd" part of this basis was taken from ref 23. It has been designed to reproduce the electric properties of  $\text{H}_2$  and first-row hydrides. To this set the 1f orbital, used by Meyer<sup>24</sup> for  $\text{H}_2$  in his study of the van der Waals constants for the  $\text{H}_2$  dimer, was added.

**Bases N, N(1d), N(3d), and N(3df).** Both the M and L bases suffer from large BSSE, caused primarily by the diffuse character of the  $\text{H}^-$  charge cloud. To circumvent the BSSE problem, a sequence of basis sets, which yield small BSSE, was constructed. This sequence is based on the Lie and Clementi's set<sup>25</sup> augmented with one diffuse s- and four p-type polarization functions and was optimized by Adams<sup>26</sup> for the electron correlation energy of both the  $\text{H}_2$  and  $\text{H}^-$  systems. This basis set is hereafter termed basis N. To the N basis, higher polarization functions of d and f symmetry were subsequently added, giving rise to the N(1d), N(3d), and N(3df) bases (cf. Tables I and VI).

**B. Optimization of Geometry.** Optimization of the energy of the lowest  $^1A'$  state of  $\text{H}_3^-$  as a function of geometry was carried out by means of the Gaussian 82 analytic energy derivative package,<sup>18</sup> at the SCF and MP2 levels. The three configurations

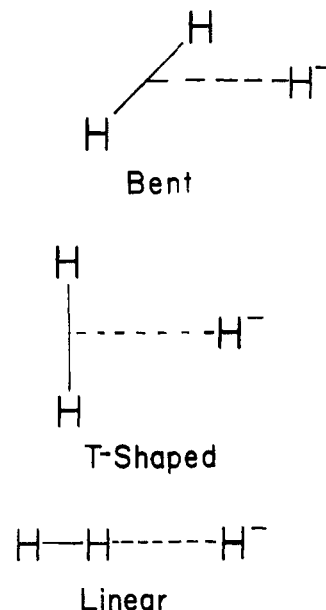


**Figure 1.** Configurations of the  $\text{H}^-(\text{H}_2)$  complex studied in this work. In the text the distances between H and H (full line) and between  $\text{H}_2$  and  $\text{H}^-$  (dashed line) are denoted  $r_{\text{HH}}$  and  $R$ , respectively. The angle between  $r_{\text{HH}}$  and  $R$  in the bent configuration is  $45^\circ$ .

studied in this work are shown in Figure 1. The bond distances  $r_{\text{HH}}$  and  $R$  are the internuclear distance of the  $\text{H}_2$  moiety and the distance from the center of mass of the  $\text{H}_2$  moiety to the  $\text{H}^-$  anion center, respectively. As was shown previously<sup>27</sup> and confirmed by our calculations, the linear configuration of  $\text{H}_3^-$  is stable with respect to angular deformation. Thus, the equilibrium geometry is linear. Further details about the bending potential energy are given in Appendix A.

At the first stage of this work, we simultaneously optimized the values of  $r_{\text{HH}}$  and of the distance between the  $\text{H}_2$  center of mass and  $\text{H}^-$  at the MP2 level with the M basis. We obtained 0.749 and 3.114 Å, respectively. The  $r_{\text{HH}}$  distance turned out to be close to the equilibrium  $r_{\text{HH}}$  distance in the isolated  $\text{H}_2$  molecule, which we found to be 0.740 Å at the MP2 level with the M basis. Using the fact that the  $\text{H}_2$  moiety is not significantly deformed by  $\text{H}^-$ , we kept  $r_{\text{HH}}$  fixed in all subsequent calculations and equal to 0.739 Å, as in the work of Hirao and Yamabe.<sup>3</sup> This restriction was found to result in a difference in the interaction energy of ca. 0.1 mhartree or 0.06 kcal/mol, which may be considered insignificant.

With  $r_{\text{HH}}$  held fixed, the value of  $R$  was optimized by means of the gradient method in Gaussian 82.<sup>18</sup> At the SCF level in basis M, we obtained  $R_c = 3.528$  Å. At the MP2 level, basis M and the extended basis N(3d) produced  $R_c$  values of 3.148 and 3.140 Å, respectively; i.e., the MP2 geometry differs substantially from the SCF geometry. These results raise the interesting questions:

(19) Van Lenthe, J. H.; van Duijneveldt-van de Rijdt, J. G. C. M.; van Duijneveldt, F. B. *Adv. Chem. Phys.* **1987**, *67*, 521.

(20) Gutowski, M.; van Duijneveldt, F. B.; Chalaśniński, G.; Piela, L. *Mol. Phys.* **1987**, *61*, 233.

(21) Van Duijneveldt, F. B. *IBM Techn. Rep.* **1971**, No. RJ945.

(22) Clark, T.; Chandrasekhar, J.; Spitznagel, G. W.; Schleyer, P. V. R. *J. Comput. Chem.* **1983**, *4*, 294.

(23) Diercksen, G. H.; Sadlej, A. J. *Theor. Chim. Acta* **1983**, *63*, 69.

(24) Meyer, W. *Chem. Phys.* **1976**, *17*, 27.

(25) Lie, G. C.; Clementi, E. *J. Chem. Phys.* **1974**, *60*, 1275.

(26) Adams, N., unpublished results.

(27) Macias, A. *J. Chem. Phys.* **1968**, *48*, 3464.

**TABLE III: The Interaction Energy and Its Components for the H<sup>-</sup>(H<sub>2</sub>) and H<sup>-</sup>⋯H<sub>2</sub> Systems (r<sub>HH</sub> = 0.739 Å; R = 3.148 Å), Obtained with Bases M, L, and N<sup>a</sup>**

(A) The H <sup>-</sup> (H <sub>2</sub> ) System, Bases M and L							
<i>i</i>	M basis			L basis			
	$\Delta E^{(i)}$	$\delta_{H_2}^{(i)}$	$\delta_H^{(i)}$	$\Delta E^{(i)}$	$\delta_{H_2}^{(i)}$	$\delta_H^{(i)}$	
SCF	-0.759	-0.012	-0.024	-0.743	-0.082	-0.055	
2	-0.403	-0.009	-0.557	-0.425	-0.090	-0.510	
3	+0.013	+5.-4	-0.075	+0.010	-0.021	+0.015	
DQ	+0.108	-3.-4	-0.040	+0.110	-0.004	-0.014	
SDQ	+0.120	-3.-4	-0.031	+0.120	-0.004	-0.011	
4	+0.059	-3.-4	-0.031	+0.056	-0.004	-0.011	
sum <sup>b</sup>	-1.091 (-1.799)	-0.021	-0.687	-1.102 (-1.860)	-0.197	-0.561	

(B) The H <sup>-</sup> ⋯H <sub>2</sub> System, Basis N Sets												
<i>i</i>	N		N(1d)			N(3d)			N(3df)			
	$\Delta E^{(i)}$	$\delta_{H_2}^{(i)}$	$\delta_H^{(i)}$	$\Delta E^{(i)}$	$\delta_{H_2}^{(i)}$	$\delta_H^{(i)}$	$\Delta E^{(i)}$	$\delta_{H_2}^{(i)}$	$\delta_H^{(i)}$	$\Delta E^{(i)}$	$\delta_{H_2}^{(i)}$	$\delta_H^{(i)}$
SCF	-0.731	-6.-5	-0.014	-0.732	-6.-5	-0.017	-0.733	-7.-4	-0.019	-0.734	-0.001	-0.027
2	-0.389	-0.014	-0.119	-0.409	-0.004	-0.067	-0.508	-0.005	-0.056	-0.508	-0.006	-0.051
3	+0.019	+2.-4	+0.089	+0.018	+2.-4	+0.068	+0.023	+0.001	+0.073	+0.019	+0.002	+0.076
DQ	+0.115	-6.-5	+0.018	+0.115	-2.-4	-0.005	+0.128	-6.-5	-0.011	+0.129	+5.-5	-0.016
SDQ	+0.131	-8.-6	+0.020	+0.132	-2.-4	-0.004	+0.146	-6.-5	-0.010	+0.146	-5.-5	-0.016
4	+0.065	-8.-6	+0.020	+0.061	-2.-4	-0.004	+0.065	-6.-5	-0.010	+0.064	-5.-5	-0.016
sum <sup>b</sup>	-1.306 (-1.060)	-0.001	-0.024	-1.063 (-1.088)	-0.004	-0.020	-1.153 (-1.171)	-0.005	-0.012	-1.159 (-1.182)	-0.005	-0.018

<sup>a</sup>Energies in kilocalories per mole. <sup>b</sup>The CP-uncorrected energies are in parentheses.

(a) How would the optimal geometry be affected by correcting for BSSE (the gradient method searches for the minimum on the CP-uncorrected curve)? (b) How would the optimal geometry be affected by allowing for higher order electron correlation effects (e.g., at the MP4 level)? To find out the answers to these questions, the values of the interaction energy, with and without BSSE, at the SCF, MP2 and MP4 levels were calculated for several *R* values in the range 2.731–4.231 Å. These energies are tabulated in Table II.

The results in Table II lead to the conclusion that correcting for the BSSE shifts  $R_e^{MP2}$  and  $R_e^{MP4}$  toward longer distances. In the worst case, the M basis shifts the  $R_e$  value by ca. 0.1 Å, a nontrivial shift. However, the potential energy surface is so flat in the region of the minimum that, at any level of theory, a change of  $\pm 0.1$  Å in *R* affects the interaction energy by only 0.001 mhartree or 0.0006 kcal/mol. Consequently, at most two digits of the previously given values of  $R_e$  should be considered as really significant. The large difference between  $R_e^{SCF}$  and  $R_e^{MP2}$ , 0.4 Å, may also be partly attributed to the flatness of the surface. Interestingly, allowing for the correlation effects at the MP4 level does not change the position of the minimum significantly; thus  $R_e^{MP2}$  is very close to  $R_e^{MP4}$ . It is worthwhile to mention here that the same situation was observed for the H<sup>-</sup>(H<sub>2</sub>O) complex.<sup>28</sup>

**C. Interaction Energy between H<sub>2</sub> and H<sup>-</sup> and the Accompanying Basis Set Effects.** The total interaction energies,  $\Delta E^{(i)}$  constituent terms, and BSSE effects obtained with various basis sets at *R* = 3.148 Å (i.e., at the BSSE uncorrected minimum) are given in Table III. The total interaction energy with the largest N(3df) basis amounts to -1.16 kcal/mol, and the accompanying BSSE is very small, 0.02 kcal/mol. In fact,  $\delta_{H_2}^{SCF}$ ,  $\delta_H^{(2)}$ , and  $\delta_H^{(3)}$  are larger in absolute value than the total  $\delta_H$ (4), but because these components have different signs, a cancellation takes place. Comparing the results obtained with different basis sets, one can conclude the following:

(a) The basis sets M and L suffer from large BSSE of 0.70 and 0.76 kcal/mol, respectively, which are dominated by the  $\delta_H^{(2)}$  component. We note that these bases are not small and were prepared in a rational, widely accepted manner. One would expect that they should therefore reproduce the dominant contributions to the interaction energy fairly well. Indeed, if the CP method is used, both the bases give a very good correlated binding energy

of -1.1 kcal/mol (see Table III). The individual  $\Delta E^{(i)}$  contributions are also close to the values obtained with our best N(3df) basis (see Table III). In contrast, if one does not correct for BSSE, the values of the total interaction energy and its components for various basis sets vary wildly and are therefore impossible to analyze.

(b) All of our N-type basis sets give very similar results and very small BSSE's, not exceeding 0.03 kcal/mol. The binding energy obtained without d functions is already quite good, -1.04 kcal/mol (basis N); the d functions are responsible for an additional 0.1 kcal/mol of stabilization. The addition of one f function did not have any significant effect, ~0.02 kcal/mol. However, this does not necessarily mean that higher polarization functions are completely negligible. In addition, one should note from Tables III that the inclusion of only one d function did not reproduce the bulk of the contributions obtained when more than one function was used. All in all, it is probably reasonable to expect that the basis-set-saturated result is ca. 0.1 kcal/mol lower. (Allowing for the deformation of H<sub>2</sub> by H<sup>-</sup> brings about a similar change of the interaction energy; see section III.B).

**D. Interpretation of the Interaction Energy at the SCF Level.**  $\Delta E^{SCF}$  represents the dominant contribution to the interaction energy, giving 65% of the total at *R*<sub>e</sub> = 3.148 Å; its contribution rapidly grows with increasing *R*. For large *R*,  $\Delta E^{SCF}$  may be interpreted as the result of electrostatic interactions of the negative charge-quadrupole and charge-induced-dipole type:<sup>29</sup>

$$\Delta E_{SCF}^{model} = \frac{q\theta^{SCF}}{R^3} - \frac{1}{2} \frac{q^2}{R^4} \left[ \bar{\alpha}^{SCF} + \frac{2}{3} (\alpha_{\parallel}^{SCF} - \alpha_{\perp}^{SCF}) \right] + O\left(\frac{1}{R^5}\right) \quad (5)$$

where *R* is measured from the center of the H<sub>2</sub> moiety as defined previously,  $\theta^{SCF}$  is the quadrupole moment of H<sub>2</sub> at the SCF level, and  $\bar{\alpha}^{SCF}$ ,  $\alpha_{\parallel}^{SCF}$ , and  $\alpha_{\perp}^{SCF}$  are the average, parallel, and perpendicular polarizabilities of H<sub>2</sub>, respectively, at the SCF level. Within our M basis set, we have  $\theta^{SCF} = 0.4843$  au,  $\alpha_{\parallel}^{SCF} = 6.461$  au,  $\alpha_{\perp}^{SCF} = 3.817$  au, and  $\bar{\alpha}^{SCF} = 4.698$  au. At *R* = 6.631 Å we can compare our fully ab initio SCF interaction energy

$$\Delta E_{SCF} = -0.372 \text{ mhartree} \quad (6a)$$

to the interaction energy predicted by the model of eq 5:

(28) Chalasiński, G.; Kendall, R.; Simons, J. *J. Chem. Phys.* **1987**, *87*, 2965.

(29) Buckingham, A. D. In *Intermolecular Interactions: from Diatomics to Biopolymers*; Pullman, B., Ed.; Wiley: New York, 1978.

$$\Delta E_{\text{SCF}}^{\text{model}} = -0.248 - 0.131 = -0.379 \text{ mhartree} \quad (6b)$$

where the first and second values correspond to the quadrupole-charge interaction and induced-dipole-charge interaction. One can see that, at this large distance, the role of induction effects is important and accounts for 36% of  $\Delta E_{\text{SCF}}$ . With decreasing  $R$  the induction term becomes even more important, and assuming that  $\Delta E_{\text{SCF}}^{\text{model}}$  is still valid, one can predict that induction becomes equal to the electrostatic terms at  $R \sim 3.72 \text{ \AA}$ . In particular, at the distance of the minimum,  $R = 3.148 \text{ \AA}$ , one has

$$\Delta E_{\text{SCF}}^{\text{model}} = -2.300 - 2.576 = -4.876 \text{ mhartrees} = -3.06 \text{ kcal/mol}$$

However, at this  $R$  the true SCF interaction is  $\Delta E_{\text{SCF}} = -0.76 \text{ kcal/mol}$ , and it is clear that the electrostatic and induction effects are canceled to a large extent by overlap and exchange effects which are included in the true  $\Delta E_{\text{SCF}}$ . Only approximately then one can envisage the SCF attraction in H<sup>-</sup>(H<sub>2</sub>) as determined by the two equally important effects: electrostatic attraction and induction attraction.

**E. Electron Correlation Contribution to the Interaction Energy.** At the equilibrium geometry,  $R_e$ , determined at the MP2 level, ( $R_e^{\text{MP2}}$ ), the total electron correlation term amounts to ca. 35% of  $\Delta E(4)$  and is dominated by  $\Delta E^{(2)}$  (cf. parts A and B of Table III). In the region of the minimum,  $\Delta E_{\text{MP}}^{(2)}$  is attractive; with increasing  $R$  it becomes less attractive and less important and amounts to +0.0081 mhartree at  $R = 6.631 \text{ \AA}$ . The above behavior of  $\Delta E_{\text{MP}}^{(2)}$  may be rationalized as follows.

It has recently been shown that the asymptotically leading contributions to  $\Delta E^{(2)}$  arise from<sup>16</sup> (a) intramolecular correlation effects on the multipole moments (quadrupole moment of H<sub>2</sub>) and polarizabilities (dipole polarizability of H<sub>2</sub>) of the constituent species. These modifications bring about related modifications of the electrostatic and induction interactions, respectively.<sup>16</sup> (b) They also arise from intermolecular correlation effects as expressed through uncoupled-Hartree-Fock (UCHF) dispersion energy.<sup>16,30</sup> In the particular case of the H<sup>-</sup>(H<sub>2</sub>) interaction, the modifications of the quadrupole moment and the dipole polarizability due to electron correlation are both negative. Consequently, the changes of the electrostatic and induction contributions (on the order of  $R^{-3}$  and  $R^{-4}$ , respectively) yield repulsive contributions. On the other hand, the dispersion term (on the order of  $R^{-6}$ ) is always attractive. For large  $R$  the terms of the lower order in  $R^{-1}$  prevail and make  $\Delta E^{(2)}$  repulsive. As  $R$  decreases, however, the dispersion term becomes important and  $\Delta E^{(2)}$  becomes attractive. Such a situation is fairly typical and has been observed for (HF)<sub>2</sub>,<sup>16</sup> (H<sub>2</sub>O)<sub>2</sub>,<sup>14</sup> and (CH<sub>3</sub>NO<sub>2</sub>)<sub>2</sub>.<sup>15</sup> Let us now examine the role of higher order correlation corrections,  $\Delta E^{(3)}$  and  $\Delta E^{(4)}$ . These terms are small compared with  $\Delta E^{(2)}$  and repulsive, both in the region of the minimum (see Table III) and for large distances: at  $R = 6.631 \text{ \AA}$ ,  $\Delta E^{(3)} = +0.0034 \text{ mhartree}$  and  $\Delta E^{(4)} = +0.0013 \text{ mhartree}$ . It is interesting to note that (see Table III)

$$\Delta E^{(3)} < \Delta E^{(4)} \quad \text{at } R_e^{\text{MP2}}$$

whereas

$$\Delta E^{(3)} > \Delta E^{(4)} \quad \text{at } R = 6.631 a_0$$

as a result of which one should be fairly cautious about assuming the same convergence of the perturbation series at all  $R$ . The rate of triple excitations is also interesting to consider. Whereas  $\Delta E_{\text{SDQ}}^{(4)}$  (no triples) is repulsive, the inclusion of triple excitations quenches about half of  $\Delta E_{\text{SDQ}}^{(4)}$ . The entire  $\Delta E^{(4)}$  is, however, very small, ca. 0.06 kcal/mol at  $R_e^{\text{MP2}}$ .

**F. Comparison with Previous Calculations.** The H<sub>3</sub><sup>-</sup> complex was studied previously by several authors.<sup>3-5,27,31</sup> The most advanced calculations were carried out by Hirao and Yamabe<sup>3</sup> and Rayez et al.<sup>5</sup> Both groups used fairly small basis sets: Hirao

TABLE IV: Comparison of Present Results with Results of Hirao and Yamabe<sup>3</sup> and Rayez et al.<sup>5</sup>

	SCF		post-SCF		method
	$R_e, \text{ \AA}$	$D_e, \text{ kcal/mol}$	$R_e, \text{ \AA}$	$D_e, \text{ kcal/mol}$	
Rayez et al. <sup>3</sup>	3.670	0.96	3.670 <sup>a</sup>	0.5	CI-SD
Hirao & Yamabe <sup>5</sup>	3.675	0.83	3.675 <sup>a</sup>	0.67 (0.59)	CI-SD
present	3.551 <sup>b</sup>	0.90 <sup>b</sup>	3.15 <sup>c</sup>	1.16 <sup>d</sup>	MP4

<sup>a</sup> $R$  was optimized only at the SCF level. <sup>b</sup>Obtained with basis M. <sup>c</sup>Obtained with basis N(3d) at the MP2 level. <sup>d</sup>Obtained with basis N(3df) at the MP4 level.

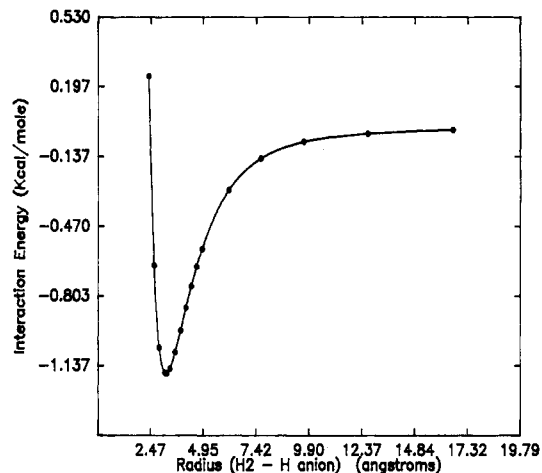


Figure 2. Interaction energy between H<sup>-</sup> and H<sub>2</sub>, ground-state, in the linear geometry defined in Figure 1. The energies were calculated at the MP4 level with the N(3d) bases.

and Yamabe used a 4-31G basis<sup>32</sup> to which they added two diffuse s and one polarization p orbitals and Rayez et al. used a STO 31G basis<sup>32</sup> augmented with one diffuse s orbital, one polarization p orbital, and two diffuse p orbitals.

In Table IV, the results of Hirao and Yamabe<sup>3</sup> and Rayez et al.<sup>5</sup> are collected and compared with ours. First, one can see that the geometries optimized at the SCF level as well as the SCF interaction energies are close to each other in all three studies. In addition, Hirao and Yamabe reported a small value of BSSE. At the post-HF level, however, the differences between our and the previous results are significant. The  $R_e$  distance differs by 0.4 Å and is due to the fact it was not previously reoptimized at the correlated level. Furthermore, the depth of the well is twice as large in our calculations as in the previous studies. Interestingly, the effect of correlation is repulsive in the works of Hirao and Yamabe and Rayez et al., whereas we obtain a significant attractive contribution.

The inadequacy of previous results at the post-HF level can be attributed to several facts: inadequate basis sets to account for correlation effects, the use of the CI-SD method, which is size-inconsistent, and, finally, BSSE. In particular, the fact that the previous authors find a repulsive contribution from the effect of electron correlation might result from the lack of polarization functions, but this effect is most likely due to the fact that the size-inconsistent methods will recover more correlation energy in the dissociation products than in the cluster.

**G. Vibrational Frequencies of H<sup>-</sup>(H<sub>2</sub>).** The algorithm available in Gaussian 82<sup>18</sup> for finding vibrational frequencies is restricted to the MP2 level (and even then is not extremely stable) and is also restricted to harmonic treatment of vibrations. Therefore, we chose to use the MP4 potential energy surface data points we calculated to generate a global potential from which to obtain the vibrational frequencies. In defense of our use of a simple one-dimensional potential for treating the bond length and stretching force constant of the H<sup>-</sup>(H<sub>2</sub>) vibrational mode, we note that the

(30) Szaba, A.; Ostlund, N. S. *J. Chem. Phys.* **1977**, *67*, 1977.

(31) Stevenson, D.; Hirschfelder, J. O. *J. Chem. Phys.* **1937**, *5*, 933. Barker, R. S.; Eyring, H.; Baker, D. A.; Thorne, C. J. *J. Chem. Phys.* **1955**, *23*, 1381. Bowen, H. C.; Linnett, J. W. *Trans. Faraday Soc.* **1964**, *39*, 1186.

(32) Ditchfield, R.; Hehre, W. J.; Pople, J. A. *J. Chem. Phys.* **1971**, *54*, 724.

**TABLE V: MP4 Vibrational Frequencies<sup>a</sup> of the Linear H<sup>-</sup>(H<sub>2</sub>), H<sup>-</sup>(HD), and D<sup>-</sup>(H<sub>2</sub>) Complexes, for the Weak Stretching Mode of H<sup>-</sup> and D<sup>-</sup><sup>b</sup>**

vibrat level, <i>V</i>	vibrat freq, cm <sup>-1</sup>		
	H <sup>-</sup> (H <sub>2</sub> )	H <sup>-</sup> (HD)	D <sup>-</sup> (H <sub>2</sub> )
0	83.5	78.6	67.8
1	213	203	180
2	302	291	264
3	358	349	324
4	388	382	364
5	403	399.8	387
6		409.9 <sup>c</sup>	400.8
7			409 <sup>c</sup>

<sup>a</sup>The SCF-level bending frequency of H<sup>-</sup>(H<sub>2</sub>) is 346 cm<sup>-1</sup>. <sup>b</sup>Well depth  $\approx$  410 cm<sup>-1</sup>. <sup>c</sup>Frequency just below threshold.

**TABLE VI: Basis Sets for Hydrogen Used in This Work<sup>a</sup>**

	exponent	contraction coeff
M Basis		
s subsets		
1	33.865 014	0.006 068
	5.094 788	0.045 316
	1.158 786	0.202 846
2	0.325 840	1.0
3	0.102 741	1.0
4	0.03	1.0
p subsets		
1	0.25	1.0
2	0.75	1.0
d subsets		
1	0.75	1.0
L Basis		
s subsets		
1	68.16	0.023 653 526
	10.246 5	0.179 766 80
	2.346 48	0.860 802 83
2	0.673 32	0.392 414 63
	0.224 66	0.656 304 47
3	0.082 217	1.0
4	0.030 338	1.0
p subsets		
	0.2	1.0
	0.7	1.0
d subsets		
	0.075	1.0
f subsets		
	0.07	1.0
N Basis		
s subsets		
	402.01	0.000 279 7
	60.242	0.002 162
	13.732 2	0.011 227 062
	3.904 51	0.044 712
	1.287 1	0.141 960 48
	0.465 544	1.0
	0.181 120 0	1.0
	0.072 791	1.0
	0.017 247 8	1.0
p subsets		
	2.273 471	1.0
	0.841 306	1.0
	0.293 257	1.0
	0.085 31	1.0
d subset		
	0.7 <sup>b,c</sup>	1.0
	0.2 <sup>b,c</sup>	1.0
	0.075	1.0
f subset		
	0.07 <sup>c</sup>	1.0

<sup>a</sup>Exponents in a<sub>0</sub><sup>-2</sup>. <sup>b</sup>Used in the N(3d) basis set only. <sup>c</sup>Used in the N(3df) basis set only.

H<sub>2</sub> molecule in the H<sup>-</sup>(H<sub>2</sub>) anion complex is not strongly perturbed by the presence of the H<sup>-</sup> ion. We used a cubic-spline fit of the MP4 data points to represent our potential. The system is

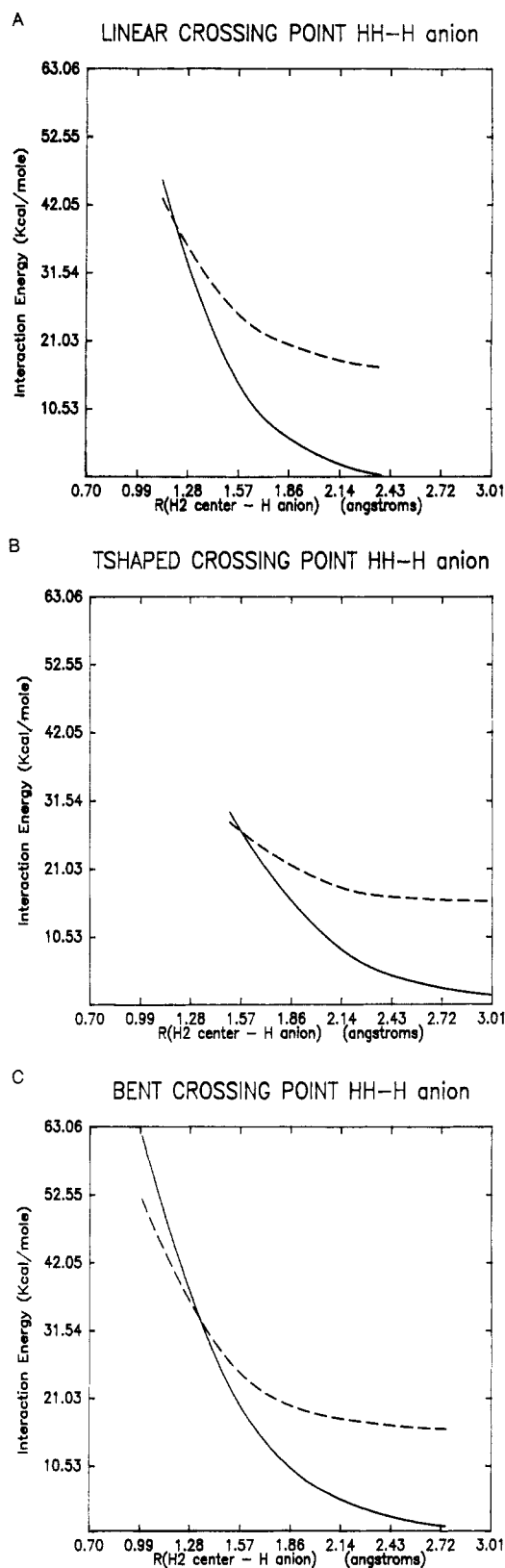


**Figure 3.** (A) Interaction energy between H<sup>-</sup> and H<sub>2</sub> (—) and H and H<sub>2</sub> (---) ground states, in the linear geometry defined in Figure 1. The energies were calculated at the MP4 level with the N(3d) basis. The zero level of energy *x* axis corresponds to the energy of H<sup>-</sup> + H<sub>2</sub>. (B) As (A) but for T-shaped geometry. (C) As (A) but for bent geometry.

therefore studied as though the H<sub>2</sub> part of the complex is a single atom having a mass twice that of ordinary hydrogen.

This potential was used to solve the radial Schrödinger equation for H<sup>-</sup>(H<sub>2</sub>) stretching motion to obtain the vibrational frequencies for this mode of the cluster. The data points used in the cubic-spline fit are the CP-uncorrected MP4 results for the N(3d) basis

TABLE VII

$j$	$x_j$	$a_j$	$b_j$	$c_j$	$d_j$
0	2.380 500 0	0.392 400 0	-7.394 400 0	6.095 426 4	1.743 094 5
1	2.630 500 0	-1.048 000 0	-4.019 856 6	7.402 747 2	-5.229 283 4
2	2.880 500 0	-1.672 000 0	-1.298 973 6	3.480 784 7	-3.530 429 6
3	3.148 100 0	-1.838 000 0	-0.194 497 3	0.646 555 8	18.316 479 5
4	3.180 500 0	-1.843 000 0	-0.094 916 8	2.426 917 6	-18.571 645 7
5	3.230 500 0	-1.844 000 0	0.008 487 7	-0.358 829 3	4.681 632 8
6	3.380 500 0	-1.835 000 0	0.216 849 1	1.747 905 5	-2.339 607 4
7	3.630 500 0	-1.708 100 0	0.652 125 4	-0.006 800 1	0.153 193 0
8	3.880 500 0	-1.543 100 0	0.677 449 1	0.108 094 7	-0.269 964 7
9	4.130 500 0	-1.371 200 0	0.680 878 1	-0.094 378 8	-0.026 934 3
10	4.380 500 0	-1.207 300 0	0.628 638 5	-0.114 579 5	-0.025 498 2
11	4.630 500 0	-1.057 700 0	0.566 567 8	-0.133 703 2	0.000 927 1
12	4.880 500 0	-0.924 400 0	0.499 890 1	-0.133 007 8	0.016 415 8
13	6.130 500 0	-0.475 300 0	0.244 319 6	-0.071 448 5	0.010 512 5
14	7.630 500 0	-0.234 100 0	0.100 933 6	-0.024 142 2	0.002 712 7
15	9.630 500 0	-0.107 100 0	0.036 917 2	-0.007 866 0	0.000 816 4
16	12.630 500 0	-0.045 100 0	0.011 763 4	-0.000 518 6	-0.000 183 7
17	16.630 500 0	-0.018 100 0			

TABLE VIII

$j$	$x_j$	$a_j$	$b_j$	$c_j$	$d_j$
0	120.000 000 0	0.858 000 0	-0.078 750 0	0.000 423 2	-0.000 002 8
1	130.000 000 0	0.110 000 0	-0.071 132 0	0.000 338 6	0.000 008 5
2	140.000 000 0	-0.559 000 0	-0.061 822 1	0.000 592 4	0.000 004 0
3	150.000 000 0	-1.114 000 0	-0.048 779 8	0.000 711 8	0.000 002 6
4	160.000 000 0	-1.528 000 0	-0.033 758 7	0.000 790 3	0.000 002 6
5	170.000 000 0	-1.784 000 0	-0.017 185 3	0.000 867 1	-0.000 000 9
6	180.000 000 0	-1.870 000 0			

set previously mentioned. This basis set has a very small BSSE, and correcting for it will not appreciably change the vibrational frequencies. The data points and the fit are shown in Figure 2. The well depth of the potential is approximately  $410 \text{ cm}^{-1}$ . All of our stretching vibrational frequency predictions are given in Table V. For the  $H^-(H_2)$  cluster, six bound vibrational levels exist at 83.5, 213, 302, 358, 388, and  $403 \text{ cm}^{-1}$ .

Because only the reduced mass changes under isotopic substitution in the  $H^-(H_2)$  complex, we were able to use the same code with the appropriate reduced mass to obtain the vibrational levels of the  $H^-(HD)$  and  $D^-(H_2)$  complexes. All results for these two complexes are shown in Table V as well. The distributions of vibrational levels of the  $H^-(HD)$  complex is very similar to that of the  $H^-(H_2)$  complex. The  $D^-(H_2)$  complex, on the other hand, has eight bound vibrational levels.

For completeness, we also include our cubic-spline interpolates for the above "stretching" potential as well as for our MP4 potential for the "bending" vibration of the complex. These results show that the linear geometry is the most stable geometry for the  $H^-(H_2)$  complex but that only  $\sim 0.823 \text{ kcal/mol}$  or  $288 \text{ cm}^{-1}$  is needed to "bend" the complex by  $40^\circ$  to  $\theta = 140^\circ$ . Thus, the bending vibration is also soft. (See Appendix A.)

We calculated the full set of  $3N - 5$  harmonic vibrational frequencies for the M basis at the SCF level of theory. These frequencies are 4519 (primarily the  $H_2$  moiety vibration), 346 (the degenerate bending mode of the cluster), and  $140 \text{ cm}^{-1}$  (the  $H^-$  stretching mode of the cluster discussed earlier). These results show that the complex's "bend" is actually stiffer than its "stretch". This order of frequencies can be understood by considering two facts. First, the cluster is not held together by a chemical bond; the attractive interaction is composed of intermolecular forces of the charge-quadrupole, charge-induced-dipole, etc. nature. The second point to note is that the parallel polarizability of the  $H_2$  moiety is greater than its perpendicular polarizability (e.g.,  $\alpha_{\parallel} = 0.934 \text{ \AA}^3$  and  $\alpha_{\perp} = 0.718 \text{ \AA}^3$ ).<sup>33</sup> As a result, the presence of

the  $H^-$  ion more easily deforms the electron cloud of  $H_2$  along the  $H_2$  bond than transverse to the bond. This then gives rise to more attractive interactions for linear geometries than for bent geometries.

*H. Energy Threshold for Electron Detachment in  $H^- + H_2$  Collisions.* Using our accurate  $H^-(H_2)$  potential, we were interested in attempting to estimate the energy threshold for electron detachment in  $H^- + H_2$  collisions. Ground-state-energy curves for  $H^-(H_2)$  and neutral  $H_3$ , in linear, typical bent, and T-shaped configurations, calculated with the N(3d) basis at the MP4 level are shown in Figure 3 in the region near their crossing. The lowest energy crossing occurs at  $R \approx 1.6 \text{ \AA}$  and lies  $27.0 \text{ kcal/mol}$  above the  $H_2 + H^-$  asymptote. Thus rather energetic collisions would be required to effect electron detachment.

#### IV. Conclusions

Our results shed new light on the controversy over the possibility of existence of the  $H^-(H_2)$  complex. It was shown that a stable (by  $1.2 \text{ kcal/mol}$ ) linear  $H^-(H_2)$  complex has a potential surface that supports six bound vibrational levels. However, proper treatment of all zero-point vibrational energies clearly shows that the complex is thermodynamically unstable relative to  $H_2$  and  $H^-$ , at 0 K. The temperature of the gaseous nebulae while not 0 K is relatively cold, roughly 50 K. Thus, it is unlikely that the  $H_3^-$  complex can be formed under these conditions. It is possible to calculate the heat of formation at 298 K from our data and by using classical approximations to account for the translational and rotational degrees of freedom.<sup>39</sup> The heat of formation for the  $H_3^-$  complex is about  $-0.4 \text{ kcal/mol}$  at 298 K. This means that there is a possibility of forming the complex at this temperature. Isotopic substitution to form  $D_3^-$  should lower the heat of formation enough, by lowering the vibrational frequencies, to make the  $D_3^-$  complex a much more viable experimental system to investigate. In addition, a threshold of  $27 \text{ kcal/mol}$  for electron detachment in  $H^- + H_2$  collisions was determined from the lowest energy crossing point of the  $H^-(H_2)$  and  $H_3$  potential surfaces. Unfor-

(33) Hirschfelder, J. O.; Curtis, C. F.; Bird, R. B. *Molecular Theory of Gases and Liquids*; Wiley: New York, 1954.

(34) Steinfeld, J. I. *Molecules and Radiation: An Introduction to Modern Molecular Spectroscopy*; MIT Press: Cambridge, MA, 1981.

(35) Davidson, E. R.; Jones, L. L. *J. Chem. Phys.* **1962**, *37*, 2966.

(36) Kolos, W.; Wolniewicz, L. *J. Chem. Phys.* **1968**, *49*, 404.

(37) Froese Fischer, C. *The Hartree-Fock Method for Atoms. A Numerical Approach*; New York, 1977.

(38) Pekeris, C. L. *Phys. Rev.* **1962**, *126*, 1470.

(39) Del Bene, J. E.; Mettee, H. D.; Frisch, M. J.; Luke, B. T.; Pople, J. A. *J. Phys. Chem.* **1983**, *87*, 3279.

tunately, to date, no experimental data is available for comparison with these predictions.

Our study of the  $\text{H}^-(\text{H}_2)$  complex is also important from the perspective of negative ion-molecule interactions. Contrary to common assumption, it was shown that electron correlation effects are of essential importance; in particular, they shorten the  $\text{H}_2\text{-H}^-$  distance by ca. 0.4 Å. They also yield ca. 40% of the interaction energy in the region of the potential. These results are analogous to our recent results on the  $\text{H}^-(\text{H}_2\text{O})$  complex.<sup>28</sup> Furthermore, both the  $\text{H}^-(\text{H}_2)$  and  $\text{H}^-(\text{H}_2\text{O})$  studies point out the importance of using extended basis sets and the CP method to remove BSSE if quantitative results are desired.

**Acknowledgment.** We acknowledge the financial support of the National Science Foundation (CHE-8511307), the U.S. Army Research Office (DAAG-2984K0086), and the donors of the Petroleum Research Fund, administered by the American Chemical Society. We also acknowledge the Harris Corp. for their generous computer system grant and the National Science Foundation for its San Diego Supercomputer time award. We also thank the San Diego Supercomputer Center for their computer time grant. G.C. also thanks the Polish Academy of Sciences within Program CPB01.12 for their partial support. We are grateful to N. Adams for providing us with his basis set for the hydrogen atom, to Dr. Dick Hilderbrandt for his help with the

Cray and SCS-40 versions of GAUSSIAN 82, and to Dr. Harvey Michels for his helpful suggestion concerning our manuscript. We are also indebted to Prof. F. W. Cagle for helpful discussion of the thermodynamic aspects of this problem.

#### Appendix A. Cubic-Spline Fits to the MP4 Surface

Both the "stretching" and "bending" potentials were interpolated by using a clamped cubic-spline function. The interpolant in the interval  $x_j \leq x < x_{j+1}$ ,  $S_j(x)$  is given by the equation

$$S_j(x) = a_j + b_j(x - x_j) + c_j(x - x_j)^2 + d_j(x - x_j)^3$$

Table VII contains the "stretching" potential interpolant where each  $x_j$  value is the  $R$  value (as defined in the main text) for each geometry of the MP4 surface. Table VIII contains the "bending" potential interpolant. In Table VIII each  $x_j$  value is the angle between the HH bond and the  $\text{HH}^-$  bond. Since  $S$  has units of millihartrees,  $a_j$  does also, and  $b_j$  has units of millihartrees per angstrom or millihartrees per degree, etc. These calculations correspond to the complex with a fixed  $r$  distance of 0.739 Å and a fixed distance between the middle H and the  $\text{H}^-$  of 2.8355 Å (this is not  $R$  as defined in the main text) at various angles. Therefore, an  $x_j$  value of 180° corresponds to the linear geometry of the  $\text{H}^-(\text{H}_2)$  complex.

Registry No.  $\text{H}^-$ , 12184-88-2;  $\text{H}_2$ , 1333-74-0.

## ESR Spectra of Matrix-Isolated $\text{LiO}_2$

D. M. Lindsay\* and D. A. Garland

Department of Chemistry, City University of New York, The City College, New York, New York 10031  
(Received: May 7, 1987)

ESR spectra assigned to  $^6\text{LiO}_2$  and  $^7\text{LiO}_2$  molecules have been produced by codepositing atomic Li plus  $\text{O}_2$  in Ar, Kr, and  $\text{N}_2$  matrices. For  $^7\text{LiO}_2$  in  $\text{N}_2$  (which gave the best spectral resolution)  $g_{xx} = 2.0077$  (2),  $g_{yy} = 2.0014$  (1), and  $g_{zz} = 2.0677$  (1) with  $A_{xx} = \pm 0.66$  (6) G,  $A_{yy} = \pm 2.67$  (3) G, and  $A_{zz} = \pm 2.24$  (5) G, where  $x$  is the  $C_2$  axis and  $y$  is perpendicular to the  $\text{LiO}_2$  plane. Point spin calculations imply a  $^2A_2$  ground state for  $\text{LiO}_2$  with isotropic and dipolar hyperfine constants:  $a = -1.42$  G and  $T_{xx} = +2.08$  G,  $T_{yy} = -1.25$  G,  $T_{zz} = -0.82$  G. The ESR data show a complete charge transfer from Li to  $\text{O}_2$  and predict that the first excited  $^2B_1$  state lies at  $5100 \pm 400 \text{ cm}^{-1}$ , in good agreement with the results of molecular structure calculations.

### Introduction

Except for  $\text{LiO}_2$ , all the alkali metal superoxides occur as crystalline solids,<sup>1</sup> readily prepared by reacting the metal with oxygen.<sup>2-4</sup> Accordingly, the gas-phase reaction of alkali metal atoms with  $\text{O}_2$  has received considerable attention, dating back to the early flame-diffusion studies of Bawn and Evans.<sup>5</sup> More recent single<sup>6,7</sup> and multiple<sup>8</sup> collision studies show that the reaction most likely proceeds via a "harpooning mechanism", involving a complete transfer of the metal valence electron to  $\text{O}_2$ . The superoxide anion has also been studied in alkali metal halide crystals<sup>9</sup> and is often used as a probe of catalytic materials.<sup>10</sup> The toxic

effect of  $\text{O}_2^-$  in biological systems is well-established,<sup>11</sup> and metal-oxygen bonding is of central importance to oxygen transport in the blood.<sup>12</sup> While the chemistry and biochemistry of metal superoxides have been actively pursued, the physical properties of these compounds have received relatively less attention. This situation may well change dramatically with the recent discovery of metal oxides exhibiting high-temperature superconductivity. In this context it is interesting to note that electron transfer between  $\text{O}_2^-$  moieties is thought to play a role in stabilizing the crystalline alkali metal superoxides and that solid  $\text{KO}_2$  is a semiconductor.<sup>13</sup>

In this paper we present electron spin resonance (ESR) spectra for individual  $\text{LiO}_2$  molecules isolated in Ar, Kr, and  $\text{N}_2$  matrices. The superoxide species were produced by codepositing atomic lithium with excess  $\text{O}_2$  and give spectra characteristic of a true ion pair,  $\text{Li}^+\text{O}_2^-$ . Computer synthesis of  $^7\text{LiO}_2$  spectra in nitrogen matrices allowed an accurate determination of all three  $^7\text{Li}$  hyperfine (hf) constants. A comparison of the measured hf with that predicted from a point spin model implies that the radical

(1) The existence of the superoxide anion ( $\text{O}_2^-$ ) in these compounds was first suggested by Pauling. See: Pauling, L. *J. Am. Chem. Soc.* **1931**, *53*, 3225. Pauling, L. *The Nature of the Chemical Bond*; Cornell University Press: Ithaca, NY, 1960.

(2) Vannerberg, N.-G. *Prog. Inorg. Chem.* **1962**, *4*, 125.

(3) Vol'nov, I. I. *Peroxides, Superoxides and Ozonides of Alkali and Alkaline Earth Metals*; Plenum: New York, 1966.

(4) Hart, W. A.; Beumel, O. F.; Whaley, T. P. *The Chemistry of Lithium, Sodium, Potassium, Rubidium, Cesium and Francium*; Pergamon: New York, 1973.

(5) Bawn, C. E. H.; Evans, A. G. *Trans. Faraday Soc.* **1937**, *33*, 1580.

(6) Lacmann, K.; Herschbach, D. R. *Chem. Phys. Lett.* **1970**, *6*, 106.

(7) Mochizuki, T.; Lacmann, K. *J. Chem. Phys.* **1976**, *65*, 3257.

(8) Kramer, S. D.; Lehmann, B. E.; Hurst, G. S.; Payne, M. G.; Young, J. P. *J. Chem. Phys.* **1982**, *76*, 3614.

(9) For example: Zeller, H. R.; Känzig, W. *Helv. Phys. Acta* **1967**, *40*, 845. Shuey, R. T.; Känzig, W. *Helv. Phys. Acta* **1967**, *40*, 873.

(10) For example: Wang, J.-X.; Lunsford, J. H. *J. Phys. Chem.* **1986**, *90*, 3890.

(11) Sawyer, D. T.; Valentine, J. S. *Acc. Chem. Res.* **1981**, *14*, 393. Fridovich, I. *Acc. Chem. Res.* **1972**, *10*, 321.

(12) Mings, D. M. P. *Nature (London), Phys. Sci.* **1971**, *230*, 154. Collman, J. P. *Acc. Chem. Res.* **1977**, *10*, 265.

(13) Khan, A. U.; Mahanti, S. D. *J. Chem. Phys.* **1975**, *63*, 2271.